



7-20-2018

# Inverse-Kinematics Proton Scattering on 42S

Lisa M. Skiles

*Ursinus College*, [liskiles@ursinus.edu](mailto:liskiles@ursinus.edu)

Follow this and additional works at: [https://digitalcommons.ursinus.edu/physics\\_astro\\_sum](https://digitalcommons.ursinus.edu/physics_astro_sum)

 Part of the [Physics Commons](#)

**Click here to let us know how access to this document benefits you.**

---

## Recommended Citation

Skiles, Lisa M., "Inverse-Kinematics Proton Scattering on 42S" (2018). *Physics and Astronomy Summer Fellows*. 19.  
[https://digitalcommons.ursinus.edu/physics\\_astro\\_sum/19](https://digitalcommons.ursinus.edu/physics_astro_sum/19)

This Paper is brought to you for free and open access by the Student Research at Digital Commons @ Ursinus College. It has been accepted for inclusion in Physics and Astronomy Summer Fellows by an authorized administrator of Digital Commons @ Ursinus College. For more information, please contact [aprock@ursinus.edu](mailto:aprock@ursinus.edu).

# Inverse-Kinematic Proton Scattering on $^{42}\text{S}$

L. M. Skiles

June 2018

## Abstract

Following an experiment at the National Superconducting Cyclotron Laboratory at Michigan State University in October 2016, we discuss preliminary analysis and results for the excited states of the isotope  $^{42}\text{S}$  via inverse-kinematics proton scattering. The experiment was conducted with the NSCL/Ursinus College hydrogen target and the GRETINA gamma-ray tracking array. We compare our results with similar measurements of other neutron-rich sulfur isotopes.

## INTRODUCTION

Nuclear shell model has been studied and documented in depth for stable isotopes, but for exotic, neutron-rich isotopes, a number of phenomena are still not widely understood. In particular, the isotope  $^{42}\text{Si}$  has been observed to have a breakdown in magicity normally present for  $N=28$  isotones. By studying the neighboring isotope  $^{42}\text{S}$ , we hope to better understand why this breakdown occurs. The neutron-rich sulfur isotopes from  $N=20$  to 28, including  $^{42}\text{S}$  ( $N=26$ ), have been previously studied via a variety of reactions. Notably, Lunderberg et al. [1] investigated the isotopes  $^{38-42}\text{S}$  via in-beam  $\gamma$ -ray spectroscopy at intermediate energies, and proposed low-energy excitation level schemes for each. However, the systematic behavior of sulfur's isotopic chain is still not well understood. Here, we report on the inverse-kinematics proton scattering of  $^{42}\text{S}$  at high energies and further explore the population of its level scheme. Additionally, we discuss the quadrupole deformation of  $^{42}\text{S}$  and combine with values calculated by Maréchal et al. [2] for even-even sulfur isotopes from  $N=20$  to 24.

## EXPERIMENT

The experiment took place at the Michigan State University National Superconducting Cyclotron Laboratory (NSCL). The primary beam consisted of 140 MeV/u  $^{48}\text{Ca}$  and was incident on a 1222 mg/cm<sup>2</sup>  $^9\text{Be}$  primary target. The resulting fragments were purified by the A1900 fragment separator [3] to form a secondary beam. After leaving the A1900, the resulting beam was then incident on the NSCL/Ursinus College Liquid Hydrogen Target, based on the design of Ryuto et al. [4], at the pivot of the S800 magnetic spectrograph [5]. The incoming beam particles were identified using the time of flight from the A1900 extended focal plane scintillator and the S800 object scintillator to the E1 scintillator, as shown in Figure 1. The reaction products downstream of the target were identified using energy loss in the S800 ion chamber and the time of flight from the S800 object scintillator to a scintillator in the focal plane of the S800, as shown in Figure 2. The GRETINA  $\gamma$ -ray tracking array [6] was focused on the liquid hydrogen target. All coincidence events between GRETINA and the S800 were collected along with downscaled S800 events.

## ANALYSIS AND RESULTS

The detection of  $\gamma$ -rays emitted by the beam passing through the target were simulated using the code UCGretina, based on the GEANT4 toolkit [7]. The NSCL/Ursinus College liquid hydrogen target contains

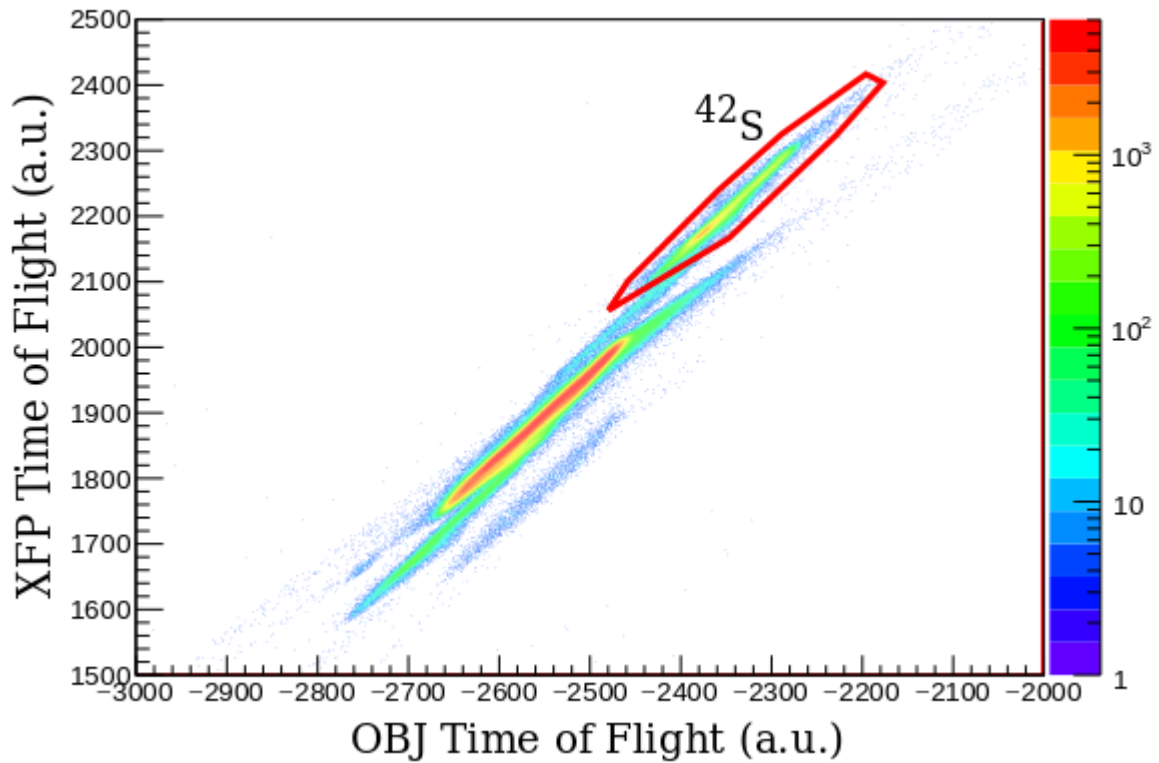


Figure 1: Incoming particle identification spectrum generated by the time of flight from the S800 object scintillator (OBJ) to the E1 scintillator in the S800 focal plane and from the A1900 extended focal plane scintillator (XFP) to the E1 scintillator.

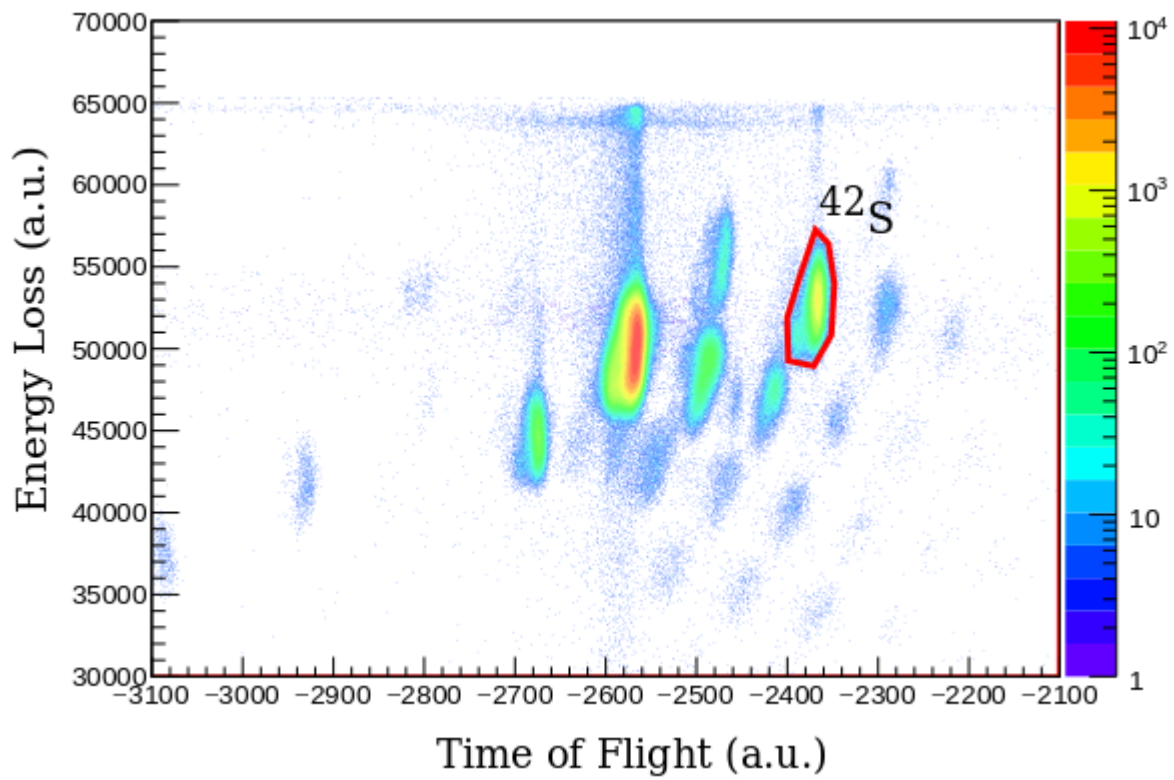


Figure 2: Outgoing particle identification spectrum generated by energy loss in the S800 ion chamber and time of flight from the S800 object scintillator to the E1 scintillator at the focal plane of the S800.

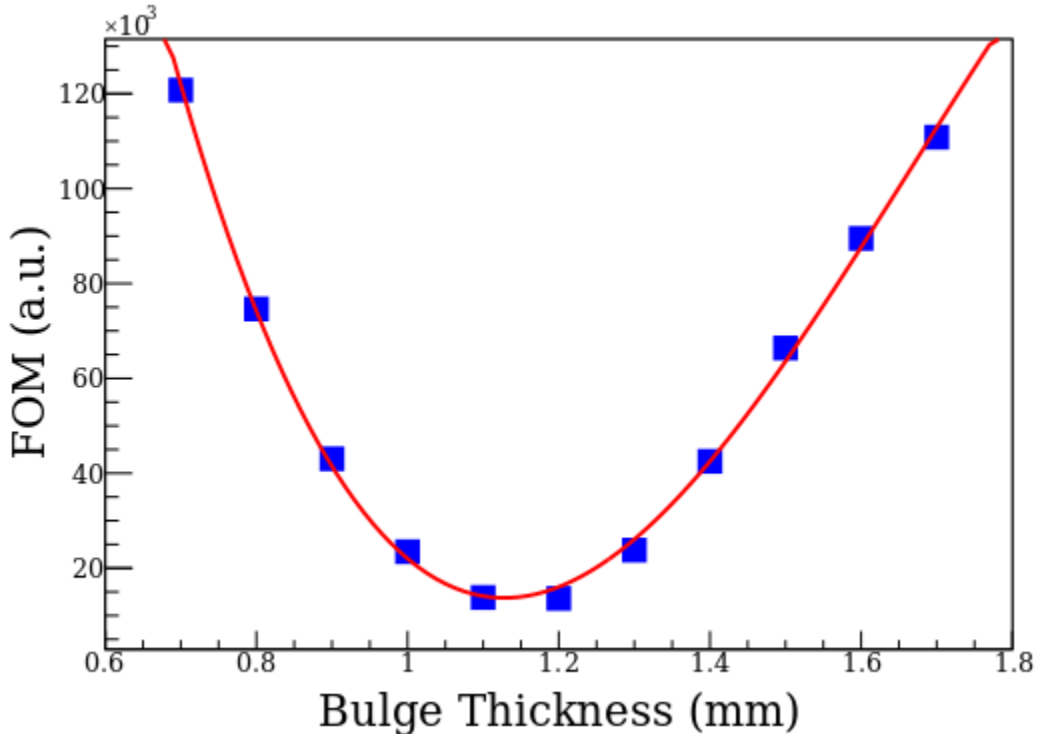


Figure 3: Simulated values for the target window bulge thickness. The red curve is a cubic polynomial fit used to minimize the function.

liquid hydrogen in a 30 mm thick aluminum cell with 125  $\mu\text{m}$  Kapton entrance and exit windows. Due to the vacuum inside the beam pipe, pressure from inside the target causes the windows to deform, resulting in extra thickness to the target. To determine the window bulge thickness, simulations varying bulge thickness were fit to the relative kinetic energy spectrum of the outgoing beam particles, as shown in Figure 3. The relative kinetic energy of the beam is given by

$$\frac{(KE - KE_o)}{(KE_o)} \quad (1)$$

where  $KE$  is the measured kinetic energy and  $KE_o$  is the central kinetic energy of the S800. Figure 4 shows simulated relative kinetic energy in blue, assuming a target window bulge thickness of 1.130(3) mm, compared to the measured relative kinetic energy spectrum in black. The resulting areal target density was 240  $\text{mg}/\text{cm}^2$ . Additionally, the offset of the target along the beam axis was determined to be 11.5(5) mm [8].

After values for bulge thickness, relative kinetic energy, and target offset were determined, simulations were run using these values with varying  $\gamma$ -ray energies near the centroids of peaks in the measured spectrum. Known and measured  $\gamma$ -ray energies for  $^{42}\text{S}$  are compared in Table 1. Additionally, the first excited state has a half life of 14.3 ps [9], which was included in the simulations. Figure 5 shows the measured  $\gamma$ -ray spectrum in black, and a fit of the Doppler corrected GEANT4 simulations, using the optimized energy values, in blue. Observed  $\gamma$ -rays correspond to those measured in previous experiments [1]. Once the  $\gamma$ -ray energies were optimized, the excited states of  $^{42}\text{S}$  were placed in into an energy level diagram, shown in Figure 6. We do not see the 2100 keV  $\gamma$  ray observed by Lunderberg et al. [1]. However, this  $\gamma$  ray de-excites the same state as the observed 2985 keV  $\gamma$  ray. Based on the relative intensities reported in Ref. [1], we conclude that the

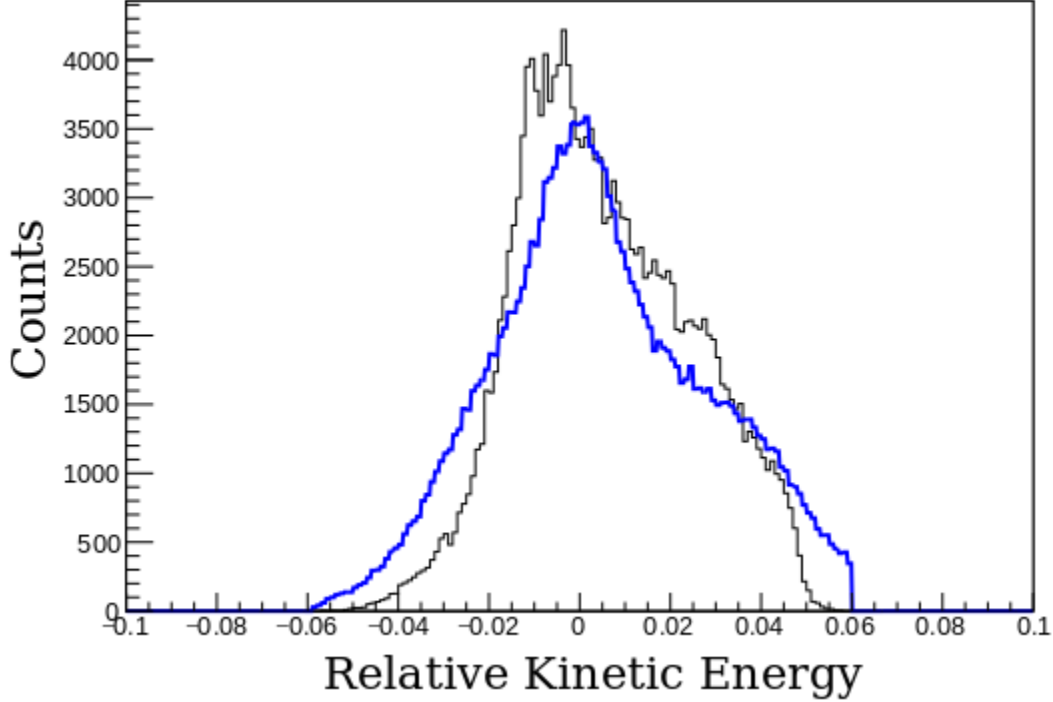


Figure 4: Relative kinetic energy spectrum of  $^{42}\text{S}$  with a simulated bulge thickness of 1.13mm.

2100 keV is below our detection threshold. We also observe a 2200 keV  $\gamma$  ray for the first time, which we are unable to place in the level scheme.

After final energies were determined, cross sections for  $^{42}\text{S}$  were calculated. The cross section for the first  $2^+$  energy level is given by

$$\sigma_{2_1^+} = \frac{N_{2_1^+}}{N_b(\rho t)} \quad (2)$$

where  $N_{2_1^+}$  is the number of  $2_1^+$  excitations,  $N_b$  is the total number of beam particles passing through the target, and  $\rho t$  is the areal particle density in protons per millibarn.  $N_{2_1^+}$  is calculated by making feeding corrections to the  $2^+ \rightarrow 0^+$  energy 903 keV for all energies that de-excite to the  $2_1^+$  state, which includes the 1840 keV and 2100 keV energies. Since the 2100 keV energy observed by Ref. [1] de-excites the  $2_2^+$  state in coincidence with the 2985 keV energy, but lies below our detection threshold, it was included in our cross section calculation. Using the 2985 keV energy and relative intensities for each of these energies as observed by Ref. [1], the ratio of 2100 keV excitations to 2985 keV excitations we would expect to see at higher resolutions was calculated and subtracted from the overall number of  $2_1^+$  excitations. Because the placement of the 2200 keV in the energy level diagram is uncertain, two cross sections, one including the 2200 keV  $\gamma$  ray and one without, were calculated and averaged. A final cross section extending over the full range of possible values was calculated to be 26(4) mb.

$E_{level}$ [keV]	Ref. [1]		Present Work	
	$J^\pi$ [ $\hbar$ ]	$E_\gamma$ [keV]	$E_\gamma$ [keV]	$I_\gamma$ [%]
0	$0^+$			
902	$2^+$	902(4)	903(2)	100(11)
2722	$(4^+)$	1820(4)	1840(12)	8(5)
3002	$(2^+)$	2100(4)	2200(25)	6(4)
		3002(4)	2985(13)	19(5)

Table 1: Energy levels, spins, parities, and  $\gamma$ -ray energies from Ref. [1].  $\gamma$ -ray energies, and intensities relative to  $2^+ \rightarrow 0^+$  transitions for the present work.

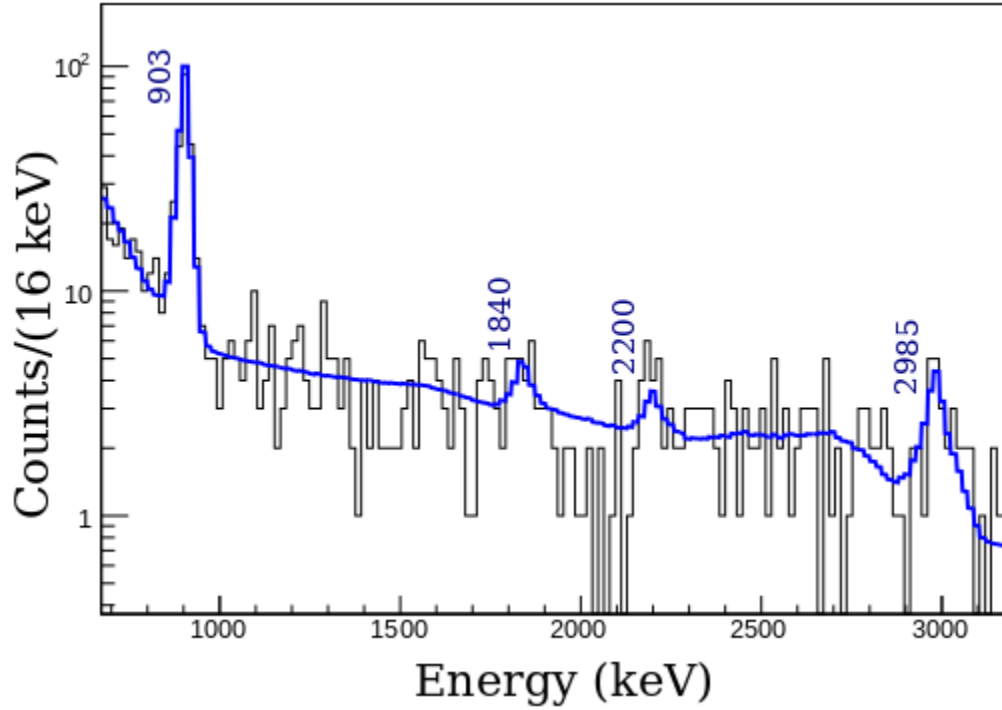


Figure 5: Doppler corrected  $\gamma$ -ray spectrum measured in coincidence with incoming and outgoing  $^{42}\text{S}$  particles. The blue curve is the fit of the GEANT4 simulations described in the text.

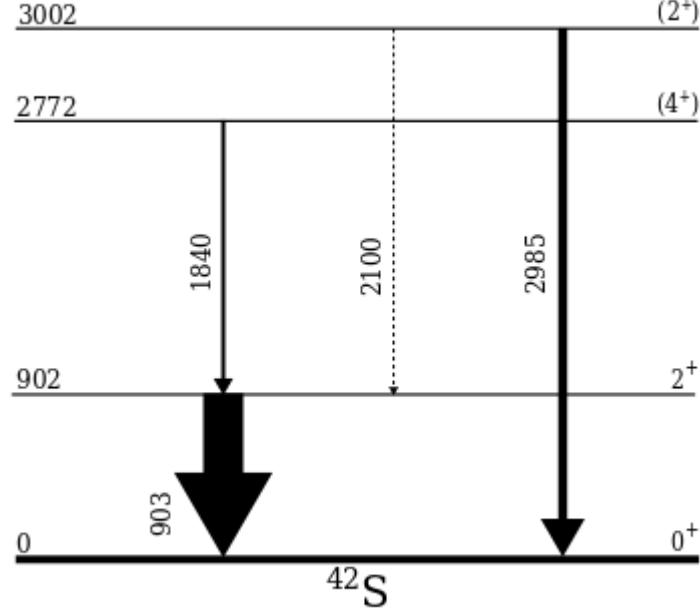


Figure 6: Proposed partial level scheme of  $^{42}\text{S}$ , including excited states populated in the present work.

## DISCUSSION

Based on the measured cross section for exciting the  $2_1^+$  state of  $^{42}\text{S}$ , its quadrupole deformation length was calculated to be 1.35(10) fm and placed into a diagram with known deformation lengths for other sulfur nuclei near the  $N=28$  shell closure [2], as shown in Figure 7. When compared to values for even-even sulfur isotopes from  $N=20$  to 28 measured by Maréchal et al. [2], our results show evidence of shell structure consistent with the nuclear shell model. There is no indication of the loss of magicity for the  $N=28$  isotope  $^{44}\text{S}$  that is observed in  $^{42}\text{Si}$ .

## References

- [1] E. Lunderberg, A. Gade, V. Bader, T. Baugher, D. Bazin, J. S. Berryman, B. A. Brown, D. J. Hartley, F. Recchia, S. R. Stroberg, D. Weisshaar, and K. Wimmer. In-beam  $\gamma$ -ray spectroscopy of S 38 – 42. *Physical Review C*, 94(6), December 2016.
- [2] F. Maréchal, T. Suomijärvi, Y. Blumenfeld, A. Azhari, E. Bauge, D. Bazin, J. A. Brown, P. D. Cottle, J. P. Delaroche, M. Fauerbach, M. Girod, T. Glasmacher, S. E. Hirzebruch, J. K. Jewell, J. H. Kelley, K. W. Kemper, P. F. Mantica, D. J. Morrissey, L. A. Riley, J. A. Scarpaci, H. Scheit, and M. Steiner. Proton scattering by short lived sulfur isotopes. *Physical Review C*, 60(3), August 1999.
- [3] D. J. Morrissey, B. M. Sherrill, M. Steiner, A. Stolz, and I. Wiedenhoever. Commissioning the A1900 projectile fragment separator. *Nuclear Instruments and Methods in Physics Research Section B: Beam Interactions with Materials and Atoms*, 204:90–96, May 2003.

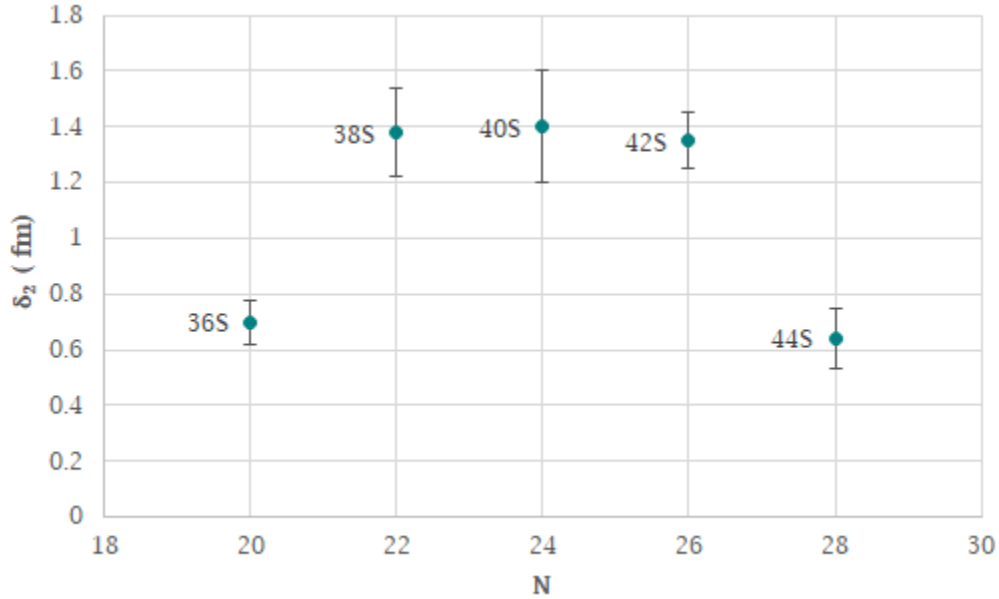


Figure 7: Proton-scattering deformation lengths of the  $2_1^+$  excitations of exotic sulfur isotopes from N=20 to 28 from Ref [2] and the present work.

- [4] H. Ryuto, M. Kunibu, T. Minemura, T. Motobayashi, K. Sagara, S. Shimoura, M. Tamaki, Y. Yanagisawa, and Y. Yano. Liquid hydrogen and helium targets for radioisotope beams at RIKEN. *Nuclear Instruments and Methods in Physics Research Section A: Accelerators, Spectrometers, Detectors and Associated Equipment*, 555(1-2):1–5, December 2005.
- [5] D. Bazin, J. A. Caggiano, B. M. Sherrill, J. Yurkon, and A. Zeller. The S800 spectrograph. *Nuclear Instruments and Methods in Physics Research Section B: Beam Interactions with Materials and Atoms*, 204:629–633, May 2003.
- [6] I.-Yang Lee. Gamma-ray energy tracking array: GRETINA. *J. Phys.: Conf. Ser.*, 420(1):012156, March 2013.
- [7] S. Agostinelli et al. GEANT4—a simulation toolkit. *Nuclear Instruments and Methods in Physics Research Section A: Accelerators, Spectrometers, Detectors and Associated Equipment*, 506(3):250–303, July 2003.
- [8] L. A. Riley. Private Communication.
- [9] J.J. Parker, I. Wiedenhöver, P.D. Cottle, J. Baker, D. McPherson, M.A. Riley, D. Santiago-Gonzalez, A. Volya, V.M. Bader, T. Baugher, D. Bazin, A. Gade, T. Ginter, H. Iwasaki, C. Loelius, C. Morse, F. Recchia, D. Smalley, S.R. Stroberg, K. Whitmore, D. Weisshaar, A. Lemasson, H.L. Crawford, A.O. Macchiavelli, and K. Wimmer. Isomeric Character of the Lowest Observed  $4^+$  State in S 44. *Physical Review Letters*, 118(5), January 2017.